Journal of Photonics for Energy

PhotonicsforEnergy.SPIEDigitalLibrary.org

Cesium lead halide ($CsPbX_3$, X = Cl, Br, I) perovskite quantum dots-synthesis, properties, and applications: a review of their present status

Soosaimanickam Ananthakumar
Jeyagopal Ram Kumar
Sridharan Moorthy Babu

SPIE.

Soosaimanickam Ananthakumar, Jeyagopal Ram Kumar, Sridharan Moorthy Babu, "Cesium lead halide ($CsPbX_3$, X = Cl, Br, I) perovskite quantum dots-synthesis, properties, and applications: a review of their present status," *J. Photon. Energy* **6**(4), 042001 (2016), doi: 10.1117/1.JPE.6.042001.

Cesium lead halide ($CsPbX_3$, X = Cl, Br, I) perovskite quantum dots-synthesis, properties, and applications: a review of their present status

Soosaimanickam Ananthakumar, Jeyagopal Ram Kumar, and Sridharan Moorthy Babu*

Anna University, Crystal Growth Centre, Sardar Patel Road, Chennai 600025, India

Abstract. Metal halide-based perovskite quantum dots (QDs) have emerged as promising materials for optoelectronics and future energy applications. Among them, cesium lead halide-based perovskite quantum dots (Cs-LHQDs) have been found to be potential luminescent candidates and alternatives for the II–VI and $I-III-VI_2$ groups semiconductor nanoparticles. These perovskites provide an excellent quantum yield (90%) larger than any other semiconductor QDs. At present, synthesis of Cs-LHQDs has been successfully achieved through a traditional colloidal-based hot-injection method and a room temperature precipitation method. Some of the interesting results in their structural, optical, and morphological properties are being analyzed to understand their energy-transfer mechanism in the colloidal state. Morphology of nanoplates, nanowires, nanocube, and nanosheets in these materials confirms their physical parameters-dependent self-assembly nature in a colloidal medium. Their potential use for light emitting diodes, photodetectors, and lasers is also highly motivated. This review provides a collective view of recent developments made in the synthesis of Cs-LHQDs and their properties. [DOI: 10.1117/1.JPE.6.042001]

Keywords: cesium lead halide perovskites; luminescent quantum dots; nonphosphinesolvents; light-emitting diode; solar cell.

Paper 16074SSMV received Jul. 3, 2016; accepted for publication Oct. 11, 2016; published online Oct. 28, 2016.

1 Introduction

Trihalide perovskites have the general structural formula AMX_3, where $A = CH_3NH_3^+$, $C_2H_5NH_3^+$, $HC(NH_2)_2^+$, and Cs^+; M = Pb, Sn, and Ge; and X = Cl, Br, I. Among them, lead-based trihalides have shown potential in recent years for display and solar cell applications. The detailed structural properties of these lead halides have been extensively investigated in the past decades.[1–5] Their intrinsic structural and optical properties such as large exciton diffusion length, good electron mobility, and stable nature against annealing (at 200°C) are under intense investigation for various optoelectronic applications. The research on lead-based and lead-free perovskites has been intensified in the last few years. Compared to lead-free perovskites, lead-based trihalide perovskites are showing more promising applications in the field of photovoltaics, light emitting diodes (LEDs), photodetectors, and lasers.

The lead-based organic–inorganic methyl ammonium hybrid perovskite $CH_3NH_3PbI_3$ and its mixed halides are showing great promise in photovoltaic applications; their effectiveness has reached over 20% within a short span of time.[6] This has triggered special attention toward the lead-based perovskite compounds. The geometry of these perovskites is decided by the parameter called the tolerance factor (t),[7] where $t = (r_A + r_X)/[2(r_B + r_X)]$, in which r_A, r_B, and r_X are the effective radii of A, B, and X ions, respectively. Replacement of the organic cation by a pure inorganic cation in hybrid perovskites influences the physical and chemical properties.

*Address all correspondence to: Sridharan Moorthy Babu, E-mail: babu@annauniv.edu

This review manuscript is also part of the section on "Breakthroughs in Photonics and Energy," highlighting primarily recent advances in the last three years.

It is under debate whether or not the organomethyl cation is a necessary one in order to make a highly efficient solar cell.

Cesium is an alkali element which has an ionic radius of 1.67 Å. When substituted in place of $CH_3NH_3^+$, it induces a strong octahedral tilting due to the lower symmetry which leads to the low bandgap (for $CsPbI_3$ it is 1.73 eV and for $CsPbCl_3$ 2.54 eV) compared to $CH_3NH_3PbCl_3$ (3.1 eV).[8] The ionic radii of the Cl^-, Br^-, I^- ions are 1.67, 1.84, and 2.07 Å, respectively.[9] In addition to this, the variation of the halide ion in perovskite matrix would strongly affect its structural and optical properties. For the third-generation photovoltaic applications, cesium-based tin perovskites ($CsSnI_3$) were effectively utilized for the solid-state dye-sensitized solar cells.[10,11]

The physical properties of bulk cesium-based lead perovskites and their amorphous type films were studied in the literature.[12–16] Continuing this, investigation of the inclusion of cesium into the methyl ammonium lead halide perovskite compound has led to improving the efficiency in solar cells from 5.1% to 7.68%.[17] Similarly, using cesium bromide (CsBr) and cesium chloride (CsCl) as modifiers, the organo lead halide perovskite-based planar heterojunction solar cells could deliver 16% and 16.8% efficiency with good stability.[18,19] A very recent analysis indicates that this efficiency increases to over 17% with the composition of $Cs_{0.2}FA_{0.8}PbI_{2.84}Br_{0.16}$.[20] Also, it has been confirmed that cesium-based perovskite solar cells have very high stability over organic–inorganic hybrid perovskite solar cells.[21] Similarly, Ripolles et al.[22] have reported that insertion of MoO_3 as the interlayer in the $CsPbI_3$ perovskite-based solar cells with the configuration of glass/FTO/bl-TiO_2/mp-TiO_2/$CsPbI_3$/P3HT/MoO_3/Au has led to an improved efficiency of 4.68% from 0.09%.

Recently, a 6.5% efficiency was achieved using $CsPb(Br_xI_{1-x})_3$ as absorber material in the device configuration of ITO/PEDOT:PSS/$CsPb(Br_xI_{1-x})_3$ (150 nm)/PCBM/BCP/Al (100 nm).[23] The thermal stability of the cesium perovskites is much higher [for instance, $CsPbBr_3$ is stable over 500°C which is higher than the $MAPbBr_3$ (~432°C)] than that of the hybrid perovskites.[24] Similarly, the black phase of $CsPbI_3$ has a higher thermal stability (over 300°C) than $MAPbI_3$ (degrades at 85°C for a long period).[25] Most of the preparation methods of perovskite lead halides reported in the literature were based on thin layer deposition and subsequent annealing treatments.[26,6] Hence, replacement of cesium in place of an organic cation in hybrid perovskites could yield many promising applications for optoelectronic devices.

Recently, cesium lead halide perovskite nanoparticles have emerged as new potential materials and show promising results for the display technology applications.[27] Surprisingly, these cesium (Cs)-based lead halide perovskite quantum dots (hereafter, Cs-LHQDs) have replaced the II–VI group semiconductor materials as potential candidates for many applications including LEDs, lasing, photodetectors, nonlinear, solar cells, and as spectrochemical probes to detect the ions.[28,29] Their superior photoluminescence properties over traditional II–VI group semiconductor materials have demonstrated the advantages of these materials for various applications. Moreover, unlike Cd-chalcogenide nanoparticles where an additional shell is required around the core (e.g., CdSe/CdS and CdSe/ZnS) to achieve more PLQYs,[30] the Cs-LHPQDs could independently produce a PLQY of up to 90%.[31] Most interestingly, the photoluminescence wavelength can be tuned from 400 to 800 nm by adjusting the ratio of the halide ions.

The nonradiative energy transfer between the quantum dots (QDs),[32] low value of full-width half maximum (FWHM) over II–VI QDs (<30 nm), and good polarized emission properties[33] are some of the notable advantages of these QDs. Ultrafast analysis of these materials reveals that the properties of the Cs-LHQDs resemble the properties of CdSe and PbSe nanoparticles.[34] Also, these Cs-LHQDs possess a low threshold, tunable wavelength, and ultrastable stimulated emission at room temperature which will be very useful for laser applications.[35] Comparative images of traditional QDs with Cs-LHPQDs are shown in Fig. 1.

These nanoparticles are synthesized in a colloidal medium as well as developed as thin film structures on glass silicon substrates and analyzed for many applications such as lasing, LEDs, and so on. It is noteworthy that when these QDs are made as a film, their optical properties such as absorption, emission, and life-time values do not changed much. Because of the high quantum yield, solution-based approaches are the focus using these Cs-LHQDs to fabricate devices such as quantum dot LEDs (QLEDs). Also, the exciton Bohr radius of the nanoparticles depends on the nature of the halide ion, i.e., it is 2.5, 3.5, and 6 nm for $CsPbCl_3$, $CsPbBr_3$, and $CsPbI_3$, respectively.[36] In the presence of an electron acceptor component, the excitons generated in

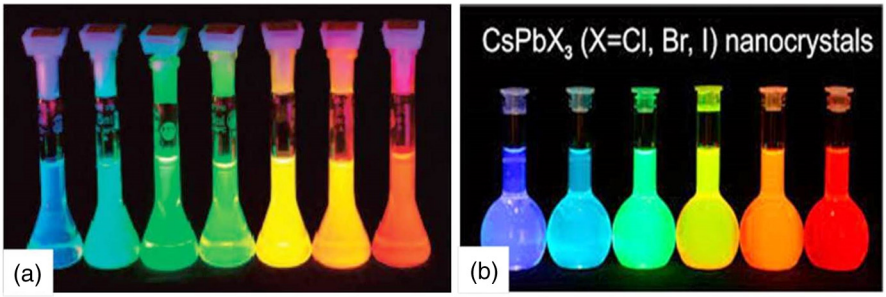

Fig. 1 Images of (a) CdSe/ZnS core–shell semiconductor QDs. Reprinted with permission from Ref. 30, © 2012 John Wiley and Sons and (b) cesium lead halide $CsPbX_3$ perovskite QDs under 365 nm UV light. Reprinted with permission from Ref. 41, © 2015 American Chemical Society.

Cs-LHQDs can efficiently be dissociated.[37] Hence, synthesizing Cs-LHQDs with a suitable methodology has been investigated in recent years.

Colloidal-based synthesis of hybrid perovskites was first reported by Schmidt et al.[38] who synthesized a stable colloidal suspension of organic–inorganic lead halide perovskites in the presence of hot coordinating solvents. Since then, various successful attempts have been made to prepare structurally tunable, highly luminescent colloidal perovskite nanoparticles.[39] Pathak et al.[40] have observed that tuning the composition of methyl and octyl ammonium cations lead to the formation of meso to nanoscale colloidal crystals with different sizes and shapes. Similarly, it was commonly observed that mixing halide ions with various ratios can be used to tune the absorption and photoluminescence emission of perovskite QDs.[41] Synthesis of perovskite QDs using solution-based approaches have been initiated very recently and considerable achievements have been made using the colloidal approach.

Colloidal-based synthesis of perovskites is encouraged due to the advantages over other methods for the application of printable photovoltaics. The colloidal chemistry used to synthesize II–VI, $I-III-VI_2$, and $I_2-II-IV-VI_4$ group semiconductor nanomaterials is being adopted for the synthesis of Cs-LHQDs. Preparation of Cs-LHQDs is carried out using either high temperature colloidal methods or room temperature assisted methods. A small tilting of octahedra (PbX_6^{4-}) and a decrease of the bond angle are the important differences of Cs-LHQDs synthesized at room temperature.[28] The nucleation and growth mechanism of these Cs-LHQDs are very fast and the entire process is completed in seconds. Brightly luminescent color tunable $CH_3NH_3PbX_3$ QDs were reported by Zhang et al.[42] at room temperature by a ligand assisted precipitation technique that has become a significant development for further improvements. Particularly, long chain amine-based solvents play a major role in the morphology evolution of perovskite nanoparticles.[43]

A recent development of polar solvent-free synthesis of colloidal hybrid perovskites has made a significant contribution to forward progress in this field.[44] In addition to the lead-based perovskites, it is possible to synthesize lead-free cesium tin halide perovskites nanoparticles using the colloidal method.[45] Seminal work carried out by Protesescu et al.[41] on the synthesis and analysis of the colloidal Cs-LHQDS $CsPbX_3$ (where X = Cl, Br, and I) has opened a new pathway toward cesium lead halide perovskite-based nanomaterials for optoelectronic applications. Most of the methods such as synthesis, ligand exchange, and measurement of optical properties of Cs-LHQDs are based on the results achieved from organic–inorganic hybrid perovskites nanoparticles. The forthcoming sections discuss the synthesis and optical properties of these materials for various potential applications.

2 Synthesis and Properties of Cesium Lead Halide Perovskite $CsPbX_3$ (X = Cl, Br, I) Nanomaterials

2.1 *Synthesis of Cesium Lead Halide Perovskite $CsPbX_3$ (X = Cl, Br, I) Quantum Dots*

The formation of lead-based perovskites for solar cells was mostly performed through thin film approaches such as sequential deposition, dip coating, and so on. Efforts on solution-based

synthesis of perovskites have appeared very recently and colloidal, emulsion-based synthesis strategies have been successively demonstrated.[46] Fortunately, the synthesis method of cesium lead trihalide perovskite nanomaterials has not been adopted on the basis of a traditional trioctylphosphine-based approach which is an extremely toxic process. Synthesis of Cs-LHQDs is carried out using a nonphosphine solvents-based colloidal method which has been adopted from the synthesis method of $I-III-VI_2$ and $I_2-II-IV-VI_4$ groups semiconductor nanomaterials. In this method, cesium-oleate complexes undergo reaction with lead halide at a high temperature (140–200°C) in the presence of nonphosphine solvents which ultimately results in the formation of cesium lead halide perovskites.

In detail, as reported by Protesescu et al.,[41] cesium carbonate (Cs_2CO_3) is placed in a three-necked flask attached with a schlenk line with the mixture of co-ordinating and noncoordinating solvents such as oleic acid (OLA) and 1-octadecene (1-ODE) and is heated strongly to 120 to 150°C under a nitrogen atmosphere. To avoid the solubility-related issues, cesium acetate (CsOAc) was also used as the cesium source.[47] During heating, the formation of a cesium-oleate complex occurs in the flask and this complex is finally converted into $CsPbX_3$ QDs when it is injected into the source of PbX_2 with OLAM/OLA/1-ODE. It was reported by the authors that the mixture of oleylamine/oleic acid (OLAM/OLA) with 1-ODE helps to solubilize the PbX_2 salt. Also, a very recent analysis shows that the addition of a mixture of OLAM/OLA helps to purify and maintain the optical properties of the Cs-LHPQDs.[48] OLAM plays an important role in the dissolution of PbX_2 salts in 1-ODE, whereas OLA provides better stability in the colloidal form.[49]

Also, the presence of a high amount of amine in the ligand shell influences the quantum yield of the Cs-LHPQDs considerably from 40% to 83%.[48] The formation of $CsPbX_3$ QDs takes place in the flask after injection of a cationic precursor and the growth continues with different morphologies when the temperature is raised to 180 to 220°C. All these processes are schematically shown in Fig. 2.

In contrast to this, it was found that a similar kind of synthetic approach was unsuccessful in the synthesis of lead-free $CsSnX_3$ (X = Cl, Br, I) nanoparticles which required the assistance of trioctyl phosphine (TOP) as a solvent to dissolve the SnX_2 precursor.[45] In fact, the use of TOP was found to be necessary to dissolve the $PbCl_2$ precursor to synthesize $CsPbCl_3$ QDs.[41,49] Unlike the semiconductor nanoparticles, synthesis of Cs-LHQDs is not carried out under heating for a long time and the reaction is quenched and brought to room temperature immediately after injecting the Cs-oleate into PbX_2-oleate mixture. According to Protesescu et al.,[41] the nucleation and growth of these Cs-LHQDs are at a very fast time scale of milliseconds to several seconds. The reaction was performed in the droplet-based microfluidic platform reaction arrangement to understand the mechanism of the reaction in detail and concluded that the reaction takes place within 1 to 5 s.[50]

Recent analysis indicates that the formation of Cs-lead halide nanoparticles takes place with byproducts such as lead oleate, oleylammonium halide, OLAM/OLA, and these byproducts can be used for the surface capping function.[48] The presence of the alkyl ammonium ion on the surface was also confirmed through H^1NMR spectroscopy.[47] The final morphology of the QDs obtained in the reaction can be varied by simply playing with the addition of new solvents and ligands. Indeed, this solvent chemistry helped to obtain a nanosheets (NSs) structure of Cs-LHQDs, which is normally a complicated one due to its cubic structure. The recent reports

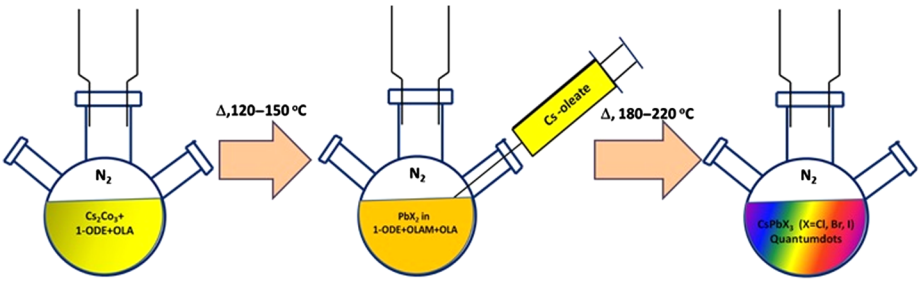

Fig. 2 Schematic diagram of the synthesis scheme of $CsPbX_3$ (X = Cl, Br, I) QDs through colloidal method.

on the formation of 2-D NSs of $CsPbBr_3$ QDs assure that such a formation can be obtained for other perovskite systems through the solution phase approach. Song et al.[51] synthesized 2-D $CsPbBr_3$ and $CsPbI_3$ NSs using long-chain alkylamines such as dodecylamine (DDA), OLAM, and n-octylamine (OTA) in addition to oleic acid as growth-directing templates. The authors obtained a thickness of 1.68 and 3.3 nm for the mono- and bilayered NSs. Interestingly, it was observed that replacing OLA by OTA lead to the formation of Cs-LHQDs nanowires (NWs).[52]

Moreover, the addition of short-chain ligands such as octanoic (or) nonanoic acid and OCT into the above reaction mixture (Cs-oleate) leads to the formation of orthorhombic $CsPbBr_3$ NSs with a thickness of ~3 nm and lateral dimensions 300 nm to a few micrometers; the lateral size can be tuned by varying the different ratios of addition of these ligands.[53] Also, the different chain lengths of carboxylic acid and alkylamine used in the reaction would also influence the final morphology of the QDs.[47] Other than these, common factors such as temperature and reaction time also influence the morphology of the QDs. For instance, a reaction temperature in the range 140 to 190°C yielded nanocube morphology, whereas the range of temperature of 130 and 90°C leads to the formation of nanoplatelets morphology.[54] Moreover, it was also possible to obtain $CsPb(Br/I)_3$ nanorod structures through this process by carefully regulating the reaction parameters.[55]

Once the synthesis process was completed, the particles were centrifuged and washed by solvents such as 1-butyl alcohol (1-butanol), tertiary butyl alcohol (3-butanol), or n-hexane. Mixed solvents such as ethyl acetate and acetone (5:1 v/v), 90% hexane, and 10% heptane were also used for this purpose.[54,56] The obtained QDs are washed with solvents upon centrifugation and produced in powder form which is used for further structural and morphological analysis. Multiple washing of Cs-LHQDs results in some adverse phenomena such as the self-soldering effect (formation of microcrystal of QDs) observed in low temperature synthesized Cs-LHQDs.[28]

Multiple washing of QDs will also lead to the removal of organic molecules present on the surface[53] and hence the particles may fuse together accordingly. Solvents used for washing may also influence the QDs' morphology. It has been observed that washing of Cs-LHQDs using butanol produces uniform morphology.[57] Traditional antisolvents such as acetone and ethanol degrade the perovskite nanoparticles which ultimately results in agglomeration due to the loss of ligands and hence photoluminescence quenching was observed after purification. Furthermore, unlike II–VI group semiconductor nanoparticles, the powdered Cs-LSHQDs could only be redispersed in limited solvents such as n-hexane and toluene. These observations clearly reveal the current setbacks that exist in solvent and ligand chemistry of Cs-LHQDs which must be eliminated. Therefore, there is a major developmental need in the field of ligand chemistry of perovskite nanoparticles, functionalization using suitable polymers, or ligands in order to improve their properties for various applications.

The utilization of polar solvents for the purification process may influence the optical properties such as photoluminescence of the prepared QDs.[48] However, solvents such as ethyl acetate and ethyl–methyl ketone can effectively help to induce as well as precipitate perovskite nanostructures and maintain the PLQY without any change.[58] Similar to this method, synthesis of $CsPbBr_3$ nanoparticles and surface treatment of the synthesized QDs using the ionic pairs namely AsS_3^{3-} and $-DDA^+$ resulted in the improvement of photoluminescence and photostability of the finally synthesized nanoparticles.[59] The chemical reaction equation of the overall formation of the $CsPbX_3$ QDs from its constituents is represented as[41]

$$2\mathrm{Cs(oleate)} + 3\mathrm{PbX_2} \xrightarrow{\Delta,140^\circ\mathrm{C}-200^\circ\mathrm{C}} 2\mathrm{CsPbX_3 nanoparticles} + \mathrm{Pb(oleate)_2}.$$

In addition to the high-temperature-based colloidal method, recent investigations reveal that highly crystalline Cs-LHQDs can be prepared at low temperatures. This strategy is based on the process of mixing the solution of precursors in good solvents (polar) [e.g., dimethyl formamide (DMF), dimethyl sulfoxide (DMSO), tetrahydrofuran] into bad solvents (nonpolar) (e.g., toluene and hexane). Sun et al.[60] synthesized highly luminescent Cs-LHQDs with different morphologies (nanospheres, nanorods, nanocubes, and nanoplates) which covered the spectral region of 380 to 693 nm by varying organic acid and amine using the room temperature reprecipitation

(RR) method. The authors also found that the shape transformation occurs through micellar transition mechanism and it influences the PL decay life time and emission spectra. A simultaneous report by Li et al.[28] highlights the synthesis of crystalline Cs-LHQDs at room temperature, in which the precursors were dissolved in either DMSO or DMF in addition to OLAM and OLA and then added into toluene. Here, the supersaturation recrystallization (SR) process was induced by transferring the precursors dissolved in good solvent into bad solvent (toluene). Interestingly, 95% of PLQY was achieved for the green emitting monoclinic $CsPbBr_3$ QDs. The authors claimed that this high PLQY was due to the self-passivation effect of the halogen (i.e., Br) which suppresses the nonradiative recombination. This room temperature-based synthesis of Cs-LHQDs has also been extended to obtain $CsPb_2Br_5$ nanoplates through a precipitation process using DMF as a solvent.[61]

Wei et al.[62] synthesized Cs-LHQDs at room temperature using long-chain fatty acids and the authors achieved 85% PLQY for the long-chain fatty acids (e.g., myristic acid and oleic acid) capped QDs and 20% to 30% PLQY for short-chain fatty acids (e.g., butyric acid) capped QDs. Other than these solvents, a very recent analysis predicts the use of methanol to obtain NWs (with a length of several micrometers to $\sim$100 μm and a thickness of $\sim$100 nm to a few micrometers) and nanoplate morphology of Cs-LHQDs at room temperature.[63] Hence, it can be concluded that the morphology of the resultant Cs-LHQDs at room temperature depends on the solvent mixture and solvent ratio used for the synthesis.

Experimental observations indicate that the perovskite nanoparticles can easily form self-assembled superstructures due to their ionic nature[45,33] and the reported morphology of the Cs-LHQDs in literature is mostly cube-like (or) square plate-like structures. This is due to the lower surface energy of {100} facets of Cs-LHQDs in solution.[64] Interestingly, Akkerman et al.[65] adopted a similar kind of procedure and obtained 2 to 5 monolayers of nanoplate-like structures of $CsPbBr_3$ by the injection of acetone into the mixture. This acetone-based formation of nanoplate-like structures was observed during the synthesis of lead-based hybrid perovskite nanostructures earlier.[66] Here, acetone plays a major role in deciding the direction of the structure by destabilizing the Cs^+ and Pb^{2+} complexes with the thickness controlled by the addition of the required amount of HBr in the solution.

In addition, the presence of 2-D confinement in the prepared nanoplates was also confirmed. A similar kind of formation of nanoplate structures of $CsPbBr_3$ was observed by Bekenstein et al.[58] when the reaction was carried out at low temperatures (90 to 130°C). The authors observed the formation of nanoplates with the lamellar structures (200 to 300 nm in size) at this lower temperature which results in the asymmetric growth of nanoplates. When the reaction temperature was raised to 150°C, nanocube-like structures with cubic phase were obtained which clearly revealed the role of temperature in tuning the morphology of Cs-LHPQDs. An interesting analysis done by Zhang et al.[67] has clearly revealed the formation of different morphologies during the synthesis of $CsPbBr_3$ and $CsPbI_3$ NWs. The initial formation of $CsPbBr_3$ nanocubes during 10 min led to the formation of NWs, NSs, and finally larger crystals during a longer time. Here, the growth of $CsPbI_3$ NWs occurs at higher temperatures (>180°C), whereas the growth of $CsPbBr_3$ was observed at 150°C.

Experimental evidence by Koolyk et al.[68] reveals the mechanism involved in the formation of Cs-LHQDs. According to the authors, the growth of the $CsPbI_3$ QDs is much faster than that of $CsPbBr_3$ QDs. Moreover, the authors observed that focusing (narrow distribution of QDs) of the $CsPbBr_3$ QDs occurs during 20 s of growth and defocusing (Ostwald ripening process of QDs) takes place while with the further increase of the growth duration. In the case of $CsPbI_3$ QDs, there was no focusing phenomena which indicates that each type of Cs-LHQDs has a different growth methodology.

2.2 *Structural, Optical, and Morphological Properties of Cs-LHQDs*

Theoretical calculations predict that the formation of the (Cl/I) mixed alloy is difficult compared with (Br/Cl) (or) (Br/I) mixtures.[69,70] Also, another theoretical analysis by Hendon et al.[71] proposed that the substitution of polyanions BF_4^- and PF_6^- in $CsPbCl_3$ instead of Cl increases the lattice parameter with more localized density of the states leading to potential interesting applications with the extension of this approach. However, further experimental support is needed to

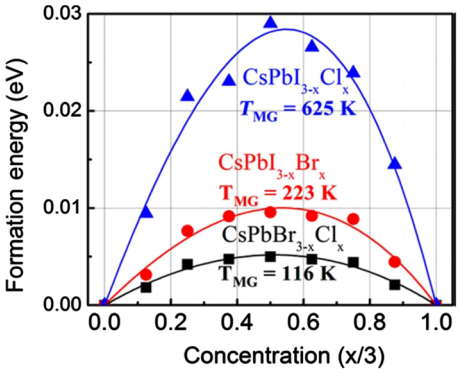

Fig. 3 Formation energies of different mixed alloys using SQS calculation. Reprinted with permission from Ref. 70, © 2014 American Chemical Society.

confirm these findings in cesium halide perovskites. The formation energies of various cesium lead halide alloys are shown in Fig. 3.

The methods used to study the structural and optical properties of these lead perovskite QDs are adopted from the studies carried out on the traditional QDs nanostructures. These Cs-LHQDs mostly exhibit a cubic structure, nevertheless, other structures such as orthorhombic and tetragonal were also observed in $CsPbBr_3$ QDs.[58,67,72] A recent investigation reveals that colloidal $CsPbBr_3$ QDs exhibit a distorted structure.[73] $CsPbI_3$ in bulk exhibits an orthorhombic phase at room temperature and is converted into cubic form when heated over 300°C; however, for nanoparticles of $CsPbI_3$, the phase transition occurs at around 100°C.[41] In other words, when temperature was lowered, $CsPbI_3$ had only one phase transition (orthorhombic-cubic, 328°C) and $CsPbBr_3$ has two phase transitions, namely orthorhombic (88°C)-tetragonal (130°C)-cubic.[67] It has also been found that the transformation of bulk crystalline $CsPbI_3$ from the δ-phase to the α-phase happens when there is an increase in temperature.[22] Inclusion of halogen into the perovskite structure strongly reflects the optical properties of Cs-LHQDs. For instance, the PL decay of the $CsPbBr_3$ QDs is much faster than that of the $CsPbI_3$ QDs and the mixed QDs, i.e., $CsPb(Br/I)_3$ QDs lie in between these two.[34,41] Similarly, the stability of the $CsPbI_3$ QDs film at ambient conditions is enhanced by additionally coating of the $CsPbCl_3$ QDs layer through formation of the $CsPbI_{3-x}Cl_x$[74] alloy.

As in the II–VI group QDs, the absorption spectra of Cs-LHPQDs are associated with the sharp excitonic peak. The peak positions depend on the nature of the halide ion and synthesis conditions. The variation in the position of the peaks was observed with the inclusion of different types of halogens (i.e., Cl, Br, I) into the structure. Also, compositionally tunable bandgap energies can be obtained using the mixture of halide ion sources (i.e., Cl/Br and Br/I). The absorption coefficient of the densely packed $CsPbBr_3$ film of 300 to 400 nm thickness was around 3.6 to 4.0 μm^{-1}.[75] Also, the absorption cross section of $CsPbBr_3$ nanocrystals was found to be nearly two times greater than that of the traditional Cd-chalcogenide nanoparticles.[76]

In the case of photoluminescence, the PL peak position also depends on other factors such as thickness of the obtained nanostructures. For example, it has been observed that the PL position shifted from 450 to 510 to 520 nm when the thickness of the NSs varied from 2.5 to 4.6 to 4.9 nm.[53] Similarly, for the $CsPbBr_3$ nanocubes, which have an edge length of 7.5 and 5.5 nm, the PL peaks were observed at 488 and 460 nm.[54] Interestingly, Swarnkar et al.[72] have found that the PL spectra width of a single $CsPbBr_3$ QDs is identical with that of the ensemble of the $CsPbBr_3$ QDs. The authors achieved an iconic value of around 90% of quantum yield for 11 nm $CsPbBr_3$ QDs which greatly surpasses the PL quantum yield of the traditional II–VI QDs. Also, it was observed that the prepared QDs were able to show temperature-independent PL peak position in the temperature range of 25 to 100°C with the absence of phenomena such as Forster resonance energy transfer which is common for II–VI group QDs. In contrast to this, Raino et al.[77] have found that a single colloidal mixed halide of $CsPb(Cl/Br)_3$ nanoparticles exhibit a lower spectral width from 25 to 1 meV full width half maximum (FWHM) than its ensemble. Transient studies show the high PLQY of $CsPbBr_3$ QDs may be due to the negligible

electron–hole trapping pathways.[37] It is to be noted that these mid-gap states are the major reason for the low PLQY of traditional QDs.

Interestingly, it was found that colloidally prepared nanoplate-like structure of Cs-LHQDs has fewer defects and surface states than the other shapes.[60,34] This clearly reveals the occurrence of a short life time from trap/surface state emissions. The distribution of these trap states has been observed using modern techniques such as first fluorescence correlation spectroscopy.[78] The FWHM of the PL spectrum tends to appear very narrow in most of the cases, which is influenced by the lead to cesium molar ratio and halide ion ratio. Moreover, this (FWHM) can be maintained if the reaction takes place between 130 and 200°C.[50] Similarly, the photoluminescence properties of these Cs-LHQDs can be tuned using the substitution of halide ions. Also, solvents such as the addition of a mixture of OLA and OLAM into the colloidal solution can be used to maintain the photoluminescent properties.[48] The origin of PL emission in lead hybrid perovskite QDs is due to the direct exciton recombination,[42] though a description in a recent report claimed it as a recombination of free electron and hole.[72]

Likewise, the origin of the PL in Cs-LHQDs was attributed to the direct bandgap transition (or) excitonic recombination.[79,54] The intensity of the PL spectrum depends on the reaction temperature, cleaning and separation conditions, and so on.[76] Moreover, the size and position of PL spectra were found to be red shifted when the synthesis temperature was increased and blue shifted when the temperature was decreased.[80] Furthermore, the nonlinear properties of these Cs-LHPQDs show that these materials could indeed be useful as better optical gain media and can be used for future nonlinear optical (NLO) devices. Colloidal $CsPbBr_3$ has shown good NLO properties and the presence of two-photon absorption (TPA) in its colloidal state has also been demonstrated.[81] Compared to other systems, in particular, optical properties, ultrafast kinetics, and applications of $CsPbBr_3$ QDs have been analyzed by many researchers in recent years. Their high carrier mobility ($\sim$4500 $cm^2\,V^{-1}\,s^{-1}$), large diffusion length (over 9.2 μm), and high PLQY (over 80%) are the attractive features of these QDs.[82] Moreover, bulk $CsPbBr_3$ has a good radiation detecting ability and good nonlinear properties.[83,84]

The photostability of the Cs-LHQDs is higher than that of organic dyes and is comparable to the cadmium chalcogenide nanoparticles. Surface passivation of the nanoparticles improves the photostability (over 36 h) of the cesium lead halide perovskites when deposited as a thin film with negligible changes in the bandgap (from 2.37 to 2.39 eV).[77] Wang et al.[35] have found that the PL spectra of the $CsPbBr_3$ QDs film depend on the pump intensities. Also, the authors observed ultrastable amplified spontaneous emission (ASE) in the thin film of perovskite layer in TPA for up to 4 months. Yakunin et al.[75] also observed a similar kind of ASE in $CsPbBr_3$ QDs (9 to 10 nm size) deposited on glass with tunable properties in most of the visible region in the range of 440 to 700 nm under low-pump thresholds down to 5 ± 1 $\mu J\,cm^{-2}$. In the same report, random lasing (i.e., without optical resonators) was also observed in the NC film of $CsPbBr_3$. In a similar way, a very lower threshold has recently been observed in $MAPbI_3$ hybrid perovskites NWs.[85]

Fu et al.[63] analyzed the lasing behavior of room temperature synthesized Cs-LHQDs NWs at 250 kHz pulsed light excitation and it was found that the lasing threshold of $CsPbBr_3$ NWs varies from 2.8 to 9 $\mu J\,cm^{-2}$. The authors were able to tune the lasing of Cs-LHQDs NWs in the entire visible region (420 to 710 nm). In addition to TPA, multiphoton absorption (MPA) was also observed in $CsPbBr_3$ QDs. Wang et al.[35] analyzed the MPA (400, 800, 1250 nm) in 9-nm sized densely packed $CsPbBr_3$ QDs films and found that just as with traditional QDs, the PL spectra of two and three-photon absorption are red shifted in comparison to the single-photon spectrum. The authors observed a very large TPA cross section of 1.2×10^5 GM, which is very beneficial for the fabrication of NLO devices. Also, the authors demonstrated the three-photon pumped green stimulated emission which is useful for biophotonic applications.

Recent analysis of the patterning of perovskite nanoparticles shows that X-ray irradiation could enhance the stability of perovskite films through the formation of C = C bonding on a ligand network.[86] Thus, additional experimental analysis of thin film of Cs-LHQDs would provide more insight to apply them to various applications.

The Cs-LHQDs can potentially serve at room temperature photon emitters and strong "photon antibunching" due to the fast auger recombination that has been observed under continuous and pulsed laser excitation.[87,77] Such a photon emitting behavior at room temperature was also

observed in a single $CsPbBr_3$ nanocrystal.[76] These findings clearly show that further progress in this area would help to understand the excellent lasing properties of Cs-LHQDs. Very recently, Makarov et al.[34] found that the auger decay is the major problem in commercializing lasing systems. The authors observed a very fast decay of Cs-LHQDs (from tens of ns to tens of ps) under high-energy laser excitation which supports the auger recombination phenomena. Though there are many similarities of Cs-LHQDs with II–VI QDs, there also exist some dissimilarities in properties such as PL blinking in small sized Cs-LHQDs.[72] Further, in depth analysis of the decay kinetics of Cs-LHQDs is expected to solve many issues related to the device applications.

2.3 *Halide Exchange in Cs-LHQDs*

In order to improve (or) tune the photoluminescence properties of $CsPbX_3$ perovskite QDs, a halide ion (anion) exchange method is being followed. This is a very characteristic method which is being followed in hybrid as well as in pure inorganic perovskite nanoparticles to tune their physical and chemical properties. In this process, the halide ion in the perovskite structure is replaced either completely or partially (in an alloy system). This exchange process is usually carried out through a gaseous phase process or intermixing of two different Cs-LHQDs solutions or soaking of a QDs layer into a lead halide source dissolved in a suitable solvent. The NWs of Cs-LHQDs with tunable compositions can be halide exchanged using OLAM/OLA at 80°C.[88] The important point is that these Cs-LHQDs can effectively function as "halide reservoirs" to exchange the halide ions with organohalides in solution.[29] Because of the large difference in the ionic radii, the exchange of the I^- to Cl^- occurs through an intermediate solid-solution formation, whereas all other halide exchange processes happen through solid-solution formation (i.e., mixture of Cl/Br, Br/I, Br/Cl, I/Br state).[89] This process has been carried out for perovskite thin films in the presence of gaseous halides as sources.[86]

Recently, Fu et al.[63] demonstrated the vapor phase anion exchange process at a reasonably low temperature (~150°C) using n-butylammonium iodide vapor. This facile "fast exchange" process is adopted to tune the optical properties of the perovskite QDs without forming the lattice (or) surface defects and without altering the crystal phase of the QDs.[36] This halide exchange method has been successfully demonstrated in organic–inorganic hybrid lead perovskite nanoparticles.[90,91]

Akkerman et al.[36] demonstrated the fast halide ion exchange process in Cs-LHQDs and proved that this process precisely maintains the structure and shape of the QDs (Fig. 4). The authors could successfully tune the absorption and PL spectra in the entire visible region using different halide ion releasing compounds (lead halides, tetrabutylammonium halides, tetraoctylammonium halides, octadecylammonium halides, oleylammonium halides, and so on). A simple halogen containing salts such as zinc halides (e.g., $ZnCl_2$ and ZnI_2) were utilized for this purpose.[60] It was also observed that the exchanged lead halide QDs had optical properties which are consistent with the directly synthesized QDs.

Ramasamy et al.[79] used this facile exchange method at room temperature using halides of lithium salts (i.e., LiI and LiCl) for the exchange/reverse exchange of $CsPbBr_3$ nanoparticles into $CsPbCl_3$ and $CsPbI_3$ nanoparticles and the authors achieved this exchange process within some seconds. Also, there was no change in the morphology structure with variation in the thickness of the exchanged products ($CsPbI_3$ NCs was thicker whereas $CsPbCl_3$ NCs was thinner than $CsPbBr_3$ NCs). It has also been observed that the halide exchange process can be achieved even in the absence of a halide source, i.e., these Cs-LHQDs could function themselves as the best halide source.

Nedelcu et al.[89] have achieved a fast anion exchange (in seconds) by using the Grignard halides and common lead halides (PbX_2) as the halide source at the temperature of 40°C.[89] Halide ion exchange is also achieved through the injection of the tetrabutyl ammonium chloride salt in toluene into the $CsPbBr_3$ in toluene.[36] More specifically, the properties of the $CsPbX_3$ QDs can be retained even after the anion exchange process.

Figure 4 shows the collective view of the process used for a halide ion exchange process of Cs-LHQDs.

Halide exchange is useful for obtaining the cubic $CsPbI_3$ phase which was normally obtained at higher temperatures. Hoffman et al.[56] used a $CsPbBr_3$ QDs film and transformed it to a cubic

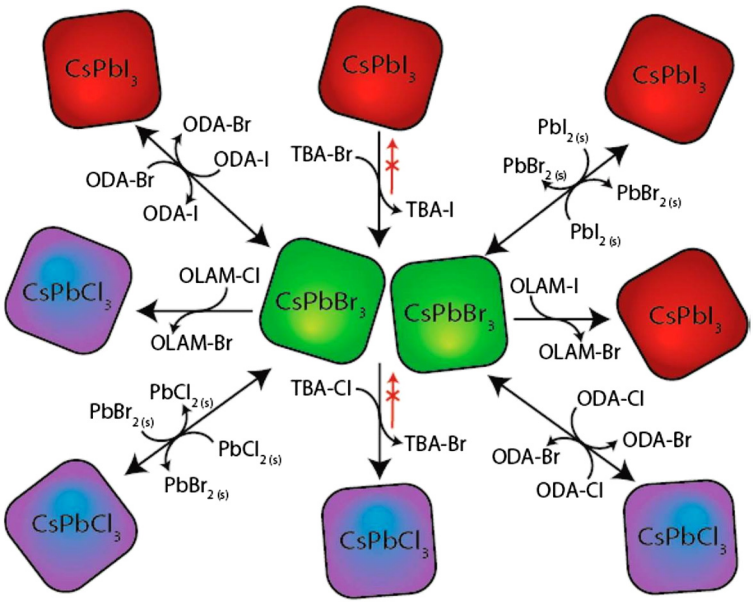

Fig. 4 The collective process of a typical anion exchange methods and precursors on $CsPbX_3$ (X = Cl, Br, I) QDs. Reprinted with permission from Ref. 36, © 2015 American Chemical Society.

$CsPbI_3$ phase by dipping the $CsPbBr_3$ QDs layer (~75-nm thickness) into the iodide precursor dissolved in OLA/OLAM/1-ODE at 75°C. Hence, the method of halide exchange process in Cs-LHQDs is very simple and this process can be avoided using the surface functionalization with thiol-based polyhedral oligomeric molecules when not required.[92]

2.4 *Applications of Cs-LHQDs*

Potential applications of the Cs-LHQDs are oriented toward LEDs, with few reports for photodetectors and solar cells. Since the polar organic molecule ($CH_3NH_3^+$) causes a hysteresis effect in organic–inorganic hybrid perovskite-based solar cell devices, replacing it with nonpolar inorganic cesium could reduce the hysteresis effect and an improvement of the efficiency can be expected. Eperon et al.[25] fabricated the first planar type solar cell device processed in an air-free atmosphere which was made by the black cubic phase of $CsPbI_3$ nanoparticles and achieved 2.9% efficiency with $V_{oc} = \sim 0.8$ V, $J_{sc} = 12$ mA/cm^2. The authors also demonstrated that the mesostructured architecture concept of $CsPbI_3$ QDs fails due to its poor transport on mesoporous titania ($\eta = 1.3\%$). Therefore, these results indicate that unlike II–VI group QDs where the sensitization on mesoporous titania (TiO_2) yields a better performance for solar cells, these Cs-LHQDs are not encouraging for the fabrication of QDs sensitized solar cells (QDSSCs).

Analysis of photovoltaic device performance of cesium perovskites by Kulbak et al.[24] indicates an equal performance in comparison with the hybrid perovskites. The authors fabricated the device configuration of FTO/d-TiO_2/mp-TiO_2/perovskite/HTM/Au using cesium and hybrid perovskites and found that both devices show an efficiency of ~6% using poly-arylamine as the hole transporting material. The low V_{oc} of the $CsPbBr_3$ (1.25 V) in comparison with $MAPbBr_3$ (1.38 V) is due to the deeper valence band of the latter. It has been experimentally observed that by coupling a molecular adsorbate with Cs-LHQDs, photon harvest in the visible spectrum can be improved toward red region which is beneficial for photovoltaic applications.[93] However, compared to the hybrid perovskites QDs and traditional II–VI group QDs, the use of Cs-LHQDs is not currently a promising path for solar cell applications currently and there are still major developments to be made in this field. On the other hand, the application of Cs-LHQDs has been found to be useful in display-related devices such as LEDs, and impressive progress has been made in this direction.[94,95]

Song et al.[80] fabricated the first quantum dot light emitting diode (QLED) based on $CsPbX_3$ QDs with the device configuration ITO/PEDOT: PSS/PVK/QDs/TPBi/LiF&Al. The authors observed luminances (i.e., the intensity of light emitted from a surface per unit area in a

given direction) of 742, 946, and 528 cd m^{-2} (cd = candela) with external quantum efficiency (EQE) values 0.07%, 0.12%, and 0.09% for the blue, green, and orange LEDs. Recent studies show that the incorporation of about an ~5-nm-thick interlayer of perfluorinated ionomer (PFI) between the hole transport layer and perovskite QDs emissive layer to avoid the charge injection barrier has led to the champion brightness value of 1377 cd m^{-2}.[57]

Prior to this, very recently Wang et al.[96] successfully designed the first liquid-type Cs-LHQDs LED in combination with a blue chip. The resultant device showed an excellent luminous efficiency of 75.5 lm/W (green), 63.4 lm/W (yellow), and 43.4 lm/W (reddish-orange) with EQE values of 14.6%, 12.4%, and 12.9%, which shows the promising avenue of high-performance liquid type Cs-LHQD LEDs. As in solar cells, the ligand OLAM and OLA present on the surface of the QDs act as the insulating barrier for the charge transport in LEDs and hence the performance of Cs-LHQD LEDs suffers. To circumvent this problem, Pan et al.[97] developed a ligand exchange strategy using a halide ion pair namely di-dodecyl dimethyl ammonium bromide (DDAB) and achieved an EQE of 3% and luminance of 330 cd m^{-2} which was higher than the device without ligand exchange. Because of the weak binding energy of the Cs-oleate and Pb-oleate components (~0.5 and ~1 eV),[49] Cs-LHQDs can be easily surface modified by other ligands by replacing the oleate from the surface.

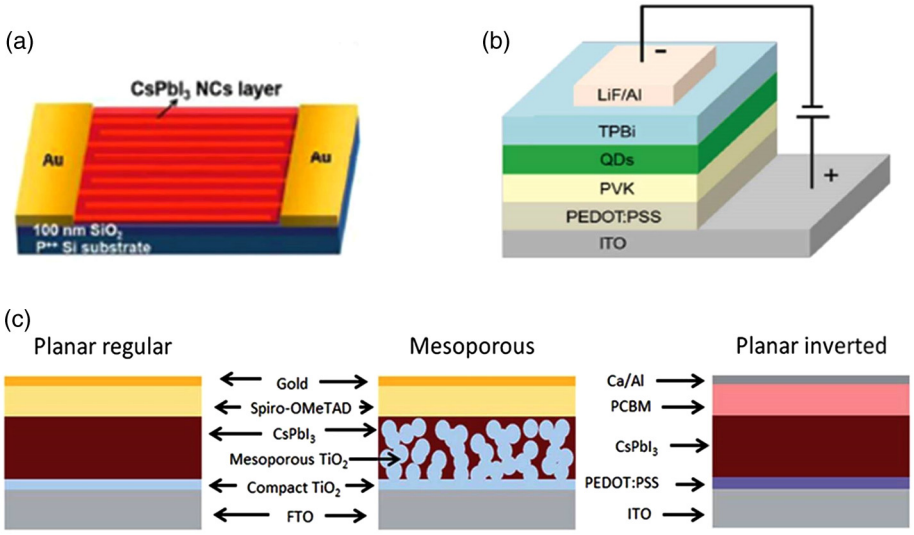

Fig. 5 Applications of $CsPbX_3$ QDs for (a) photo detector. Reprinted from Ref. 79 with the permission of The Royal Society of Chemistry. (b) LEDs. Reprinted with permission from Ref. 80, © 2015 John Wiley and Sons. (c) Different architectures of solar cells configuration using $CsPbI_3$ as photoactive material. Reprinted with permission from Ref. 25, © 2015 American Chemical Society.

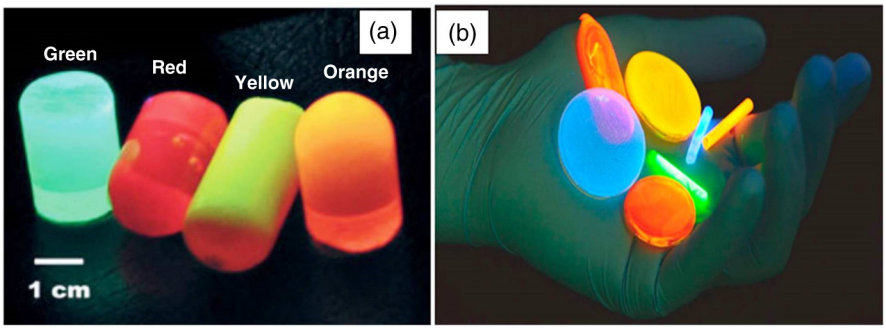

Fig. 6 (a) CdTe nanoparticles/PS nanocomposites (365 nm). Reprinted with permission from Ref. 99, © 2003 John Wiley and Sons. (b) $CsPbX_3$ nanoparticles/polymethylmethacrylate (PMMA) nanocomposites under the UV light (365 nm). Reprinted with permission from Ref. 41, © 2015 American Chemical Society.

Zhou et al.[64] have found that the modification of Ce^{3+}:YAG using red-emitting $CsPbBrI_2$ QDs enhances its luminescence efficiency of 58 lm W^{-1} at the operation current of 20 mA. Similarly, due to the short-exciton recombination life time (<10 ns), $CsPbBr_3$ QDs have extremely high modulation bandwidth (491 MHz) over traditional phosphors which is much useful for color converting applications.[98] Surface modification of Cs-LHQDs has also arisen as a powerful technique to utilize them for optoelectronic applications. Huang et al.[92] have found that the modification of Cs-LHQDs using mercaptopropyl isobutyl-polyhedral oligomeric silsesquioxane (POSS) enhances their resistance to water which can be used for the single-layer down converting WLEDs. Hence, the use of Cs-LHQDs for LEDs has been proven as ideal with an emission performance better than the II–VI group QDs. The collective applications of Cs-LHQDs in various optoelectronics area are shown in Fig. 5.

Table 1 Some of the important differences between Cs-LHPQDs and II–VI, I – III – VI_2 QDs.

S. No.	Cs-LHPQDs	II–VI and I – III – VI_2 group QDs
1	More ionic in nature, size distribution, and temperature has less influence in broadening the PL spectra. But a small blue shift was observed in $CsPbBr_3$ NWs when increasing the temperature	Size distribution and temperature have greater influence on the UV and PL spectra. UV and PL move toward red with increasing the size
2	PL blinking does not often happen for the QDs having the size of less than 10 nm and exciton self-trapping was observed due to ionic behavior	PL blinking occurs in the small-sized nanoparticles and this phenomena is very characteristic one
3	Synthesis is performed using nonphosphine solvents. With exceptional cases, sparse use of phosphine solvents are reported during the preparation of $CsPbCl_3$ QDs	Synthesis is performed using phosphine, nonphosphine, and aqueous solvents
4	Alloying of nanoparticles using different halide ions is possible to tune the absorption and emission spectrum	Alloying of anionic species (S, Se, Te) influence the optical properties
5	PL spectrum is tuned by the halogen exchange process and 90% of quantum yield has been achieved and the emission intensity is independent of the excitation power	PL spectrum can be tuned through the inclusion of other elements and achieved quantum yield is <90% and can be improved with the addition of a shell layer
6	Effect of ligand exchange is not studied currently only halide ion exchange being analyzed	Ligand exchange process influences the optical properties
7	Mostly, cubic phase formation has been achieved during the synthesis which varies with temperature and the role of solvent in phase transformation is limited. Other phases include tetragonal and orthorhombic	The phase formation is mostly dependent on the synthesis conditions, nature of solvents adopted for the synthesis (e.g., 1-DDT motivates wurtzite structure whereas elemental sulfur motivates formation of zinc blende structure in $CuInS_2$ NPs synthesis)
8	Spectral tuning depends on the halogen used during the synthesis and size regulation is not a constraint as like II–VI group QDs	Spectral tuning is mostly dependent on the temperature and different sizes of the nanoparticles, i.e., different emission can be achieved through the same batch of synthesis
9	The stability of the Cs-LHPQDs is high even after the continuous illumination of UV light (365 nm)	The stability is affected and decreases by the illumination of the UV light (365 nm) owing to deformation of ligand species present on the surface of the nanoparticles
10	When redispersed, stability in nonpolar solvents is limited but much stable than hybrid perovskite nanoparticles	Redispersion improve stability and highly stable for longer time in polar and nonpolar solvents

In addition to the high-temperature synthesized Cs-LHQDS, the room temperature synthesized nanoparticles by Li et al.[28] have also been found to be experimentally suitable for white light emitting device applications. The authors observed that room temperature synthesized Cs-LHQDs have shown the CIE co-ordination value of standard white color and a wide gamut of pure colors.

Song et al.[51] fabricated a photodetector using $CsPbBr_3$ NSs and the device possessed good stability and good light switching behavior (light on/off ratio $> 10^3$), good peak responsivity (517 nm at 5 V), EQE of 53% (at 515 nm under 10 V bias), and rise and decay times of 19 and 25 μs which excellently surpassed the silicon-based photodetector. Interestingly, a $CsPb(Br/I)_3$ nanorods-based photodetector device fabricated by Tang et al.[55] shown rise and decay times of 0.68 and 0.66 s under the laser excitation of 532 nm (optical power 20 mW) and photosensitivity value of 10^3 which clearly illustrates the promising use of one dimensional Cs-LHQDs for such applications.

Like the II–VI group luminescent semiconductor nanoparticles, these Cs-LHQDs also can produce transparent, translucent QDs/polymer nanocomposites. II–VI group semiconductor nanoparticles-based transparent polymer nanocomposites have already been made using many polymers such as poly methyl methacrylate (PMMA), polystyrene (PS), and so on[99–102] [Fig. 6(a)]. With the help of solvents such as chloroform ($CHCl_3$), the perovskite nanoparticles also displayed stable composites with PMMA which clearly shows the applications of a variety of polymers[28,41,87] [Fig. 6(b)].

However, use of Cs-LHQDs in combination with the insulating polymer is not encouraged for the LED applications. Kim et al.[49] have found a solution for this problem and through their novel centrifugal casting approach to replace the excessive ligands. The authors were able to cast highly luminescent, crack-free $CsPbBr_3$ as a film on the glass substrate and the cast films showed identical absorption and emission spectra in their position in comparison with a nanoperovskite solution. A similar kind of optical resemblance behavior in life time and PLQY was observed by Yakunin et al.[75] in 400- to 530-nm thicknesses of $CsPbBr_3$ NC film with refractive indices 1.85 to 2.30. Very recently, it was observed that Cs-LHQDs with mixed compositions and hybrid with traditional QDs (hybrid perovskite-chalcogenide QDs) could form a better color conversion layer on the top of the UV LED.[103] This shows that further understanding of Cs-LHQDs film formation and converting them for display applications would provide insight in this field. The selected differences between the II–VI and $I-III-VI_2$ QDs and Cs-LHPQDs are tabulated in Table 1.

3 Conclusion and Future Perspectives

Cs-LHQDs have emerged as promising materials to replace the binary cadmium chalcogenides and copper-based ternary luminescent nanomaterials in display devices. Their good stability at higher temperature and withstanding ability against moisture over hybrid perovskites have opened a new platform in research fields. Despite its many advantages in terms of applications over the organic–inorganic hybrid perovskites, II–VI, and $I-III-VI_2$ QDs, many optical and structural issues of the $CsPbX_3$ QDs have yet to be resolved for optoelectronic applications. The current hurdles associated with the precipitation and washing of Cs-LHQDs have to be overcome with new strategies. Also, the suitable ligand and solvent chemistry for these QDs needs to be developed to utilize them effectively for other applications such as bioimaging.

The photochemistry and physics of the excited states are to be well scrutinized to visualize the physical phenomena associated with the system. Also, the trap states present in the material are to be analyzed in detail to identify their exact role in the photoluminescence properties. Further analysis in transient studies would resolve the lifetime phenomena associated with the Cs-LHPQDs. The problems in achieving practical devices using these materials such as auger recombination also need to be suppressed. Also, additional properties such as surface modification, a core–shell type configuration with suitable band position of materials would solve many issues in the future and can help to extend this to various applications. Certainly, the fundamental physics of these QDs is very interesting and can open a new door to lead-free nanomaterials in future.

The already existing literature in research findings of II–VI QDs would support the revelation of many new structural and optical behaviors of Cs-LHQDs. It is expected that future study on these subjects would explore and perhaps disclose many mysteries in Cs-LHQDs.

Acknowledgments

The authors sincerely thank DST-SERI (DST/TMC/SERI/FR/90) Govt. of India for funding the research. S. Ananthakumar and J. Ram Kumar sincerely thank the Ministry of New and Renewable Energy (MNRE), Govt. of India for providing fellowship under National Renewable Energy Fellowship (NREF) scheme for the doctoral studies.

References

1. D. B. Mitzi et al., "Conducting tin halides with a layered organic-based perovskite structure," *Nature* **369**, 467–469 (1994).
2. D. B. Mitzi et al., "Transport, optical, and magnetic properties of the conducting halide perovskite $CH_3NH_3SnI_3$," *J. Solid State Chem.* **114**(1), 159–163 (1995).
3. D. B. Mitzi et al., "Structurally tailored organic-inorganic perovskites: optical properties and solution-processed channel materials for thin-film transistors," *Chem. Mater.* **13**(10), 3728–3740 (2001).
4. Z. Xu et al., "Semiconducting perovskites $(2\text{-}XC_6H_4C_2H_4NH_3)_2SnI_4$ (X = F, Cl, Br): steric interaction between the organic and inorganic layers," *Inorg. Chem.* **42**(6), 2031–2039 (2003).
5. D. B. Mitzi, "Synthesis, structure, and properties of organic-inorganic perovskite and related materials," Chapter 1 in *Progress in Inorganic Chemistry*, Vol. **48**, K. D. Karlin and D. B. Mitzi, Eds., pp. 1–121, John Wiley & Sons, Canada (1999).
6. L. Yang et al., "Recent progress and challenges of organometal halide perovskite solar cells," *Rep. Prog. Phys.* **79**(2), 026501 (2016).
7. G. Kieslich, S. Sun, and A. K. Cheetham, "An extended tolerance factor approach for organic-inorganic perovskites," *Chem. Sci.* **6**, 3430–3433 (2015).
8. D. Sapori et al., "Quantum confinement and dielectric profiles of colloidal nanoplatelets of halide inorganic and hybrid organic-inorganic perovskites," *Nanoscale* **8**, 6369–6378 (2016).
9. W.-J. Yin et al., "Halide perovskite materials for solar cells: a theoretical review," *J. Mater. Chem. A* **3**, 8926–8942 (2015).
10. U. Bach and T. Daeneke, "A solid advancement for dye-sensitized solar cells," *Angew. Chem. Int. Ed.* **51**, 10451–10452 (2012).
11. N. Chander, P. S. Chandrasekhar, and V. K. Komarala, "Solid state plasmonic dye sensitized solar cells based on solution processed perovskite $CsSnI_3$ as the hole transporter," *RSC Adv.* **4**, 55658–55665 (2014).
12. K. Heidrich, H. Kunzel, and J. Treusch, "Optical properties and electronic structure of $CsPbCl_3$ and $CsPbBr_3$," *Solid State Commun.* **25**(11), 887–889 (1978).
13. G. Murtaza and I. Ahmad, "First principle study of the structural and optoelectrnic properties of cubic perovskites $CsPbM_3$ (M = Cl, Br, I)," *Phys. B: Condens. Matter* **406**(17), 3222–3229 (2011).
14. S. Kondo et al., "Extremely photo-luminescent microcrystalline $CsPbX_3$ (X = Cl, Br) films obtained by amorphous-to-crystalline transformation," *Curr. Appl Phys.* **4**(5), 439–444 (2004).
15. K. Heidrich, H. Kunzel, and J. Treusch, "Optical properties and electronic structures of $CsPbCl_3$ and $CsPbBr_3$," *Solid State Commun.* **25**, 887–889 (1978).
16. S. Hirotsu and T. Suzuki, "Critical thermodynamic properties around the successive phase transitions of $CsPbBr_3$ and $CsPbCl_3$," *Ferroelectrics* **20**, 179–180 (1978).
17. H. Choi et al., "Cesium-doped methylammonium lead iodide perovskite light absorber for hybrid solar cells," *Nano Energy* **7**, 80–85 (2014).
18. W. Li et al., "Enhanced UV-light stability of planar heterojunction perovskite solar cells with cesium bromide interface modification," *Energy Environ. Sci.* **9**, 490–498 (2016).

19. W. Li et al., "Effect of cesium chloride modification on the film morphology and UV-induced stability of planar perovskite solar cells," *J. Mater. Chem. A* **4**, 11688–11695 (2016).
20. C. Yi et al., "Entropic stabilization of mixed A-cation ABX_3 metal halide perovskites for high performance perovskite solar cells," *Energy Environ. Sci.* **9**, 656–662 (2016).
21. M. Kulbak et al., "Cesium enhances long-term stability of lead bromide perovskite-based solar cells," *J. Phys. Chem. Lett.* **7**(1), 167–172 (2016).
22. T. S. Ripolles et al., "Efficiency enhancement by changing perovskite crystal phase and adding a charge extraction interlayer in organic amine-free perovskite solar cells based on cesium," *Sol. Energ. Mat. Sol. Cells* **144**, 532–536 (2016).
23. R. E. Beal et al., "Cesium lead halide perovskites with improved stability for tandem solar cells," *J. Phys. Chem. Lett.* **7**(5), 746–751 (2016).
24. M. Kulbak, D. Cahen, and G. Hodes, "How important is the organic part of lead halide perovskite photovoltaic cells? Efficient $CsPbBr_3$ cells," *J. Phys. Chem. Lett.* **6**(13), 2452–2456 (2015).
25. G. E. Eperon et al., "Inorganic cesium lead iodide perovskite solar cells," *J. Mater. Chem. A* **3**, 19688–19695 (2015).
26. N.-G. Park, "Perovskite solar cells: an emerging photovoltaic technology," *Mater. Today* **18**(2), 65–72 (2015).
27. Z. Bai and H. Zhong, "Halide perovskite quantum dots: potential candidates for display technology," *Sci. Bull.* **60**(18), 1622–1624 (2015).
28. X. Li et al., "$CsPbX_3$ quantum dots for lighting and displays: room temperature synthesis, photoluminescence superiorities, underlying origins and white light-emitting diodes," *Adv. Fun. Mater.* **26**, 2435–2445 (2016).
29. T. L. Doane et al., "Using perovskite nanoparticles as halide reservoirs in catalysis and as spectrochemical probes of ions in solution," *ACS Nano* **10**, 5864–5872 (2016).
30. A. L. Rogach et al., "Organization of matter on different size scales: monodisperse nanocrystals and their superstructures," *Adv. Fun. Mater.* **12**, 653–664 (2012).
31. S. Bai, Z. Yuan, and F. Gao, "Colloidal metal halide perovskite nanocrystals: synthesis, characterization, and applications," *J. Mater. Chem. C* **4**, 3898–3904 (2016).
32. C. De Weerd et al., "Energy transfer between inorganic perovskite nanocrystals," *J. Phys. Chem. C* **120**, 13310–13315 (2016).
33. D. Wang et al., "Polarized emission from $CsPbX_3$ perovskite quantum dots," *Nanoscale* **8**, 11565–11570 (2016).
34. N. S. Makarov et al., "Spectral and dynamical properties of single excitons, biexcitons, and trions in cesium-lead halide perovskite quantum dots," *Nano Lett.* **16**(4), 2349–2362 (2016).
35. Y. Wang et al., "All-inorganic colloidal perovskite quantum dots: a new class of lasing materials with favourable characteristics," *Adv. Mater.* **27**(44), 7101–7108 (2015).
36. Q. A. Akkerman et al., "Tuning the optical properties of cesium lead halide perovskite nanocrystals by anion exchange reactions," *J. Am. Chem. Soc.* **137**(32), 10276–10281 (2015).
37. K. Wu et al., "Ultrafast interfacial electron and hole transfer from $CsPbBr_3$ perovskite quantum dots," *J. Am. Chem. Soc.* **137**(40), 12792–12795 (2015).
38. L. C. Schmidt et al., "Nontemplate synthesis of $CH_3NH_3PbBr_3$ perovskite nanoparticles," *J. Am. Chem. Soc.* **136**(3), 850–853 (2014).
39. Y. Hassan et al., "Structure-tuned lead halide perovskite nanocrystals," *Adv. Mater.* **28**(3), 566–573 (2016).
40. S. Pathak et al., "Perovskite crystals for tunable white light emission," *Chem. Mater.* **27**(23), 8066–8075 (2015).
41. L. Protesescu et al., "Nanocrystals of cesium lead halide perovskites ($CsPbX_3$, X = Cl, Br, and I): novel optoelectronic materials showing bright emission with wide color gamut," *Nano Lett.* **15**(6), 3692–3696 (2015).
42. F. Zhang et al., "Brightly luminescent and color-tunable colloidal $CH_3NH_3PbX_3$ (X = Br, I, Cl) quantum dots: potential alternatives for display technology," *ACS Nano* **9**(4), 4533–4542 (2015).
43. J. A. Sichert et al., "Quantum size effect in organometal halide perovskite nanoplatelets," *Nano Lett.* **15**(10), 6521–6527 (2015).

44. O. Vybornyi, S. Yakunin, and M. V. Kovalenko, "Polar-solvent-free colloidal synthesis of highly luminescent alkylammonium lead halide perovskite nanocrystals," *Nanoscale* **8**, 6278–6283 (2016).
45. T. C. Jellicoe et al., "Synthesis and optical properties of lead-free cesium tin halide perovskite nanocrystals," *J. Am. Chem. Soc.* **138**, 2941–2944 (2016).
46. H. Huang et al., "Emulsion synthesis of size-tunable $CH_3NH_3PBr_3$ quantum dots: an alternative route toward efficient light-emitting diodes," *ACS Appl. Mater. Interfaces* **7**(51), 28128–28133 (2015).
47. A. Pan et al., "Insight into the ligand-mediated synthesis of colloidal $CsPbBr_3$ perovskite nanocrystals: the role of organic acid, base and cesium precursors," *ACS Nano* (2016).
48. J. D. Roo et al., "Highly dynamic ligand binding and light absorption coefficient of cesium lead bromide perovskite nanocrystals," *ACS Nano* **10**(2), 2071–2081 (2016).
49. Y. Kim et al., "Efficient luminescence from perovskite quantum dot solids," *ACS Appl. Mater. Interfaces* **7**(45), 25007–25013 (2015).
50. I. Lignos et al., "Synthesis of cesium lead halide perovskite nanocrystals in a droplet-based microfluidic platform: fast parametric space mapping," *Nano Lett.* **16**(3), 1869–1877 (2016).
51. J. Song et al., "Monolayer and few-layer all-inorganic perovskites as a new family of two-dimensional semiconductors for printable optoelectronic devices," *Adv. Mater.* **28**, 4861–4869 (2016).
52. D. Zang et al., "Synthesis of composition tunable and highly luminescent cesium lead halide nanowires through anion-exchange reactions," *J. Am. Chem. Soc.* **138**, 7236–7239 (2016).
53. J. Shamsi et al., "Colloidal synthesis of quantum confined single crystal $CsPbBr_3$ nanosheets with lateral size control up to the micrometer range," *J. Am. Chem. Soc.* **138**, 7240–7243 (2016).
54. V. K. Ravi et al., "Excellent green but less impressive blue luminescence from $CsPbBr_3$ perovskite nanocubes and nanoplatelets," *Nanotechnology* **27**, 325708 (2016).
55. X. Tang et al., "All-inorganic perovskite $CsPb(Br/I)_3$ nanorods for optoelectronic application," *Nanoscale* **8**, 15158–15161 (2016).
56. J. B. Hoffman, A. L. Schleper, and P. V. Kamat, "Transformation of sintered $CsPbBr_3$ nanocrystals to cubic $CsPbI_3$ and gradient $CsPbBr_xI_{3-x}$ through halide exchange," *J. Am. Chem. Soc.* **138**(27), 8603–8611 (2016).
57. X. Zhang et al., "Enhancing the brightness of cesium lead halide perovskite nanocrystal based green light-emitting devices through the interface engineering with perfluorinated ionomer," *Nano Lett.* **16**(2), 1415–1420 (2016).
58. Y. Bekenstein et al., "Highly luminescent colloidal nanoplates of perovskite cesium lead halide and their oriented assemblies," *J. Am. Chem. Soc* **137**(51), 16008–16011 (2015).
59. J. Pan et al., "Air-stable surface-passivated perovskite quantum dots for ultra-robust, single-and two-photon-induced amplified spontaneous emission," *J. Phys. Chem. Lett.* **6**(24), 5027–5033 (2015).
60. S. Sun et al., "Ligand-mediated synthesis of shape-controlled cesium lead halide perovskite nanocrystals via reprecipitation process at room temperature," *ACS Nano* **10**(3), 3648–3657 (2016).
61. K-H. Wang et al., "Large scale synthesis of highly luminescent perovskite-related $CsPb_2Br_5$ nanoplatelets and their fast anon exchange," *Angew. Chem. Int. Ed.* **55**, 8328–8332 (2016).
62. S. Wei et al., "Room-temperature and gram-scale synthesis of $CsPbX_3$ (X = Cl, Br, I) perovskite nanocrystals with 50-85% photoluminescence quantum yields," *Chem. Commun.* **52**, 7265–7268 (2016).
63. Y. Fu et al., "Broad wavelength tunable robust lasing from single-crystal nanowires of cesium lead halide perovskites ($CsPbX_3$, X = Cl, Br, I)," *ACS Nano* **10**(8), 7963–7972 (2016).
64. J. Zhou et al., "Inorganic halide perovskite quantum dot modified YAG-based white LEDs with superior performance," *J. Mater. Chem. C* **4**, 7601–7606 (2016).
65. Q. A. Akkerman et al., "Solution synthesis approach to colloidal cesium lead halide perovskite nanoplatelets with monolayer-level thickness control," *J. Chem. Soc.* **138**(3), 1010–1016 (2016).

66. P. Tyagi, S. M. Arveson, and W. A. Tisdale, "Colloidal organohalide perovskite nanoplatelets exhibiting quantum confinement," *J. Phys. Chem. Lett.* **6**(10), 1911–1916 (2015).
67. D. Zhang et al., "Solution-phase synthesis of cesium lead halide perovskite nanowires," *J. Am. Chem. Soc.* **137**(29), 9230–9233 (2015).
68. M. Koolyk et al., "Kinetics of cesium lead halide perovskite nanoparticles growth; focusing and de-focusing of size distribution," *Nanoscale* **8**, 6403–6409 (2016).
69. W.-J. Yin et al., "Halide perovskite materials for solar cells: a theoretical review," *J. Mater. Chem. A* **3**, 8926–8942 (2015).
70. W.-J. Yin, Y. Yan, and S.-H. Wei, "Anomalous alloy properties in mixed halide perovskites," *J. Phys. Chem. Lett.* **5**(21), 3625–3631 (2014).
71. C. H. Hendon et al., "Assesment of polyanion (BF_4^- and PF_6^-) substitutions in hybrid halide perovskites," *J. Mater. Chem. A* **3**, 9067–9070 (2015).
72. A. Swarnkar et al., "Colloidal $CsPbBr_3$ perovskite nanocrystals: luminescent beyond traditional quantum dots," *Angew. Chem. Int. Ed.* **54**(51), 15424–15428 (2015).
73. P. Cottingham and R. L. Brutchey, "On the crystal structure of colloidally prepared $CsPbBr_3$ quantum dots," *Chem. Commun.* **52**, 5246–5249 (2016).
74. S. Dastidar et al., "High chloride doping levels stabilize the perovskite phase of cesium lead iodide," *Nano Lett.* **16**, 3563–3570 (2016).
75. S. Yakunin et al., "Low-threshold amplified spontaneous emission and lasing from colloidal nanocrystals of ceasium lead halide perovskites," *Nat. Commun.* **6**, 1–8 (2015).
76. F. Hu et al., "Superior optical properties of perovskite nanocrystals as single photon emitters," *ACS Nano* **9**(12), 12410–12416 (2015).
77. G. Raino et al., "Single cesium lead halide perovskite nanocrystals at low temperature: fast single-photon emission, reduced blinking, and exciton fine structure," *ACS Nano* **10**, 2485–2490 (2016).
78. S. Seth et al., "Fluorescence blinking and photoactivation of all-inorganic perovskite nanocrystals $CsPbBr_3$ and $CsPbBr_2I$," *J. Phys. Chem. Lett.* **7**(2), 266–271 (2016).
79. P. Ramasamy et al., "All-inorganic cesium lead halide perovskite nanocrystals for photodetector applications," *Chem. Commun.* **52**, 2067–2070 (2016).
80. J. Song et al., "Quantum dot light-emitting diodes based on inorganic perovskite cesium lead halides ($CsPbX_3$)," *Adv. Mater.* **27**(44), 7162–7167 (2015).
81. W-G. Lu et al., "Nonlinear optical properties of colloidal $CH_3NH_3PbBr_3$ and $CsPbBr_3$ quantum dots: a comparison study using Z-scan technique," *Adv. Opt. Mater.* (2016).
82. G. R. Yettapu et al., "Terahertz conductivity within colloidal $CsPbBr_3$ perovskite nanocrystals: remarkably high carrier mobilities and large diffusion lengths," *Nano Lett.* **16**, 4838–4848 (2016).
83. C. C. Stoumpos et al., "Crystal growth of the perovskite semiconductor $CsPbBr_3$: a new material for high-energy radiation detection," *Cryst. Growth Des.* **13**, 2722–2727 (2013).
84. D. J. Clark et al., "Polarization-selective three-photon absorption and subsequent photoluminescence in $CsPbBr_3$ single crystal at room temperature," *Phys. Rev. B* **93**, 195202 (2016).
85. H. Zhu et al., "Lead halide perovskite nanowire lasers with low lasing thresholds and high quality factors," *Nat. Mater.* **14**, 636–642 (2015).
86. F. Palazon et al., "X-ray lithography on perovskite nanocrystals films: from patterning with anion-exchange reactions to enhanced stability in air and water," *ACS Nano* **10**(1), 1224–1230 (2016).
87. Y-S. Park et al., "Room temperature single-photon emission from individual perovskite quantum dots," *ACS Nano* **9**(10), 10386–10393 (2015).
88. D. Zhang et al., "Synthesis of composition tunable and highly luminescent cesium lead halide nanowires through anion-exchange reactions," *J. Am. Chem. Soc.* **138**, 7236–7239 (2016).
89. G. Nedelcu et al., "Fast anion-exchange in highly luminescent nanocrystals of cesium lead halide perovskites ($CsPbX_3$, X = Cl, Br, I)," *Nano Lett.* **15**(8), 5635–5640 (2015).
90. D. M. Jang et al., "Reversible halide exchange reaction of organometal trihalide perovskite colloidal nanocrystals for full-range band gap tuning," *Nano Lett.* **15**(8), 5191–5199 (2015).

91. G. Li et al., "Reversible anion exchange reaction in solid halide perovskites and its implication in photovoltaics," *J. Phys. Chem. C* **119**(48), 26883–26888 (2015).
92. H. Huang et al., "Water resistant $CsPbX_3$ nanocrystals coated with polyhedral oligomeric silsesquioxane and their use as solid state luminophores in all-perovskite white light-emitting devices," *Chem. Sci.* **7**, 5699–5703 (2016).
93. P. Maity, J. Dana, and H. N. Ghosh, "Multiple charge transfer dynamics in colloidal $CsPbBr_3$ perovskite quantum dots sensitized molecular adsorbate," *J. Phys. Chem. C* (2016).
94. H. C. Yoon et al., "Study of perovskite QD down-converted LEDs and six-color white LEDs for future displays with excellent color performance," *ACS Appl. Mater. Interfaces* **8**(28), 18189–18200 (2016).
95. J. H. Oh et al., "Evaluation of new color metrics: guidelines for developing narrow-band red phosphors for WLEDs," *J. Mater. Chem. C* **4**, 8326–8348 (2016).
96. P. Wang et al., "Multicolor fluorescent light-emitting diodes based on cesium lead halide perovskite quantum dots," *Appl. Phys. Lett.* **109**, 063106 (2016).
97. J. Pan et al., "Highly efficient perovskite-quantum-dot light-emitting diodes by surface engineering," *Adv. Mater.* **28**, 8718–8725 (2016).
98. I. Dursun et al., "Perovskite nanocrystals as a color converter for visible light communication," *ACS Photonics* **3**, 1150–1156 (2016).
99. H. Zhang et al., "From water-soluble CdTe nanocrystals to fluorescent nanocrystal-polymer transparent composites using polymerizable surfactants," *Adv. Mater.* **15**(10), 777–780 (2003).
100. H. Zhang et al., "Manipulation of semiconductor nanocrystal growth in polymer soft solids," *Soft Matter* **5**, 4113–4117 (2009).
101. S. Mohan et al., "Green synthesis and yellow emitting PMMA-CdSe/ZnS quantum dots nanophosphors," *Mater. Sci. Semicond. Process.* **39**, 587–595 (2015).
102. H. Song and S. Lee, "Photoluminescent (CdSe)ZnS quantum dot-polymethylmethacrylate polymer composite thin films in the visible spectral range," *Nanotechnology* **18**, 055402 (2007).
103. F. Palazon et al., "Polymer-free films of inorganic halide perovskite nanocrystals as UV-to-white color conversion layers in LEDs," *Chem. Mater.* **28**, 2902–2906 (2016).

Soosaimanickam Ananthakumar received his master's degree in chemistry from the University of Madras, Loyola College, Chennai, India, in 2006, and his PhD in 2016 under the guidance of Dr. S. Moorthy Babu at Crystal Growth Centre, Anna University, Chennai, India. He has authored more than 10 publications in international journals. His research interests include synthesis of semiconductor nanoparticles by colloidal method, fabrication and analysis of dye sensitized, quantum dot sensitized, and perovskite solar cells.

Jeyagopal Ram Kumar received his bachelor's and master's degrees in chemistry from Bharathidasan University, St. Joseph's College, Trichy, India, and his PhD from Anna University, Chennai, India, in 2015 under the guidance of Dr. S. Moorthy Babu. He has authored more than 10 publications in international journals. His research interests are the development of ternary and quaternary chalcopyrite nanoparticles through the colloidal and hydrothermal method for solar cell applications.

Sridharan Moorthy Babu is a professor at the Crystal Growth Centre and director at the Centre for Nanoscience and Technology, Anna University, Chennai, India. He has authored more than 130 publications in international journals. His research interests include development of inorganic semiconductor nanomaterials for dye-sensitized, quantum dot-sensitized, and perovskite solar cells, synthesis of inorganic rare earth doped nanophosphors for LED applications and growth and characterization of tungstate-based bulk crystals for laser and nonlinear applications.